Chemical Vapor Deposition of Ruthenium and Osmium Thin Films Using (Hexafluoro-2-butyne)tetracarbonylruthenium and -osmium

Yoshihide Senzaki,† Wayne L. Gladfelter,*,† and Fred B. McCormick‡

Department of Chemistry, University of Minnesota, Minneapolis, Minnesota 55455, and 3M Corporate Research Laboratories, St. Paul, Minnesota 55144

Received June 14, 1993. Revised Manuscript Received September 23, 1993®

The known mononuclear ruthenium complex Ru(hfb)$(CO)_4$, where hfb stands for hexafluoro-2-butyne, has a vapor pressure of 1.5 Torr at 25 °C and forms reflective ruthenium thin films by chemical vapor deposition (CVD) using H_2 carrier gas with a growth rate of 21 nm/min at 500 °C. The resistivity of a ruthenium film having a grain size of 60 nm was 22 μΩ cm. Auger electron spectroscopy (AES), X-ray photoelectron spectroscopy (XPS), and X-ray diffraction (XRD) analyses indicated that the films were pure, polycrystalline ruthenium (<1% C, O, or F). Scanning electron microscopy and XRD analyses revealed that the deposition temperature and the presence of H_2 gas affect the microstructure and the resistivity of the films. Os(hfb)-$(CO)_4$ afforded polycrystalline osmium thin films using H_2 as a carrier gas. A growth rate of 14 nm/min, a resistivity of 81 μΩ cm, and a grain size of 20 nm were found for depositions conducted at 600 °C. XPS analysis indicated that the film consists of 84% Os, 7% O, and 9% C. The new dinuclear metal complexes $M_2[\mu\text{-}\eta^1\text{:}\eta^1\text{:}\eta^4\text{-}C_4(CF_3)_4](CO)_6$ (M = Ru, Os) were formed from M(hfb)$(CO)_4$ during the CVD processes conducted in the absence of H_2 gas at the temperature range 150–300 °C.

Introduction

Although chemical vapor deposition (CVD) of transition-metal thin films has been of interest for applications in the electronics industry, relatively few studies have been reported thus far on the CVD of ruthenium and osmium thin films.[1-3] Ruthenium and osmium both have a hexagonal close-packed structure and exhibit several physical and chemical properties that make them interesting for applications such as contact materials or diffusion barriers in microelectronic devices.[4-13] In addition to their high melting points (2310 °C for Ru and 3050 °C for Os) and metallic conductivities (electrical resistivities ρ = 7.6 μΩ cm for Ru and 8.1 μΩ cm for Os at 0 °C, respectively), they are both mechanically strong and chemically inert.[14] Also, it has been reported that thin films consisting of multilayers of cobalt/ruthenium, prepared by sputtering techniques, exhibit novel magnetic properties.[15]

Earlier work on the CVD of ruthenium utilized Ru(acac)$_3$ derivatives (acac = acetylacetonate),[7,16,17] $Ru_3(CO)_{12}$,[7] or $(\eta^5\text{-}C_5H_5)_2Ru$[7,18] to produce either ruthenium or ruthenium oxide films depending on the carrrier gas. Although the purest metallic films were prepared from $Ru_3(CO)_{12}$, the relatively low vapor pressure of these precursors limits their utility for film growth. Unfortunately, the more volatile alternative, $Ru(CO)_5$, has a low stability which limits its use as a precursor. The use of tri- or hexafluoroacetylacetonate ligands increased the volatility of the Ru(acac)$_3$ precursors and led to higher Ru CVD growth rates. Difficulties due to the instability of the Ru(acac)$_3$ precursors were noted and organic byproducts, presumably oligomers of the acetylacetonate ligands, contaminated the reactor.[17]

Only one example of CVD of osmium thin films has been reported.[19] The precursor, $OsCl_4$, underwent considerable decomposition at the temperatures required for its volatilization (550 °C), and a high substrate temperature (1250 °C) was required for the deposition of osmium. Similar to the ruthenium analog, the more volatile Os-$(CO)_5$ is unstable which limits its use as a precursor.

The report of the synthesis of stable, volatile (hexafluoro-2-butyne)carbonyl complexes of Ru (1) and Os (2)[20] prompted us to study their use as precursors for the chemical vapor deposition of the metals.[21]

† University of Minnesota.
‡ 3M Corporate Research Laboratories.
• Abstract published in *Advance ACS Abstracts,* November 1, 1993.

(1) Green, M. L.; Levy, R. A. *J. Met.* **1985**, *37*, (6), 63.
(2) Cooke, M. J. *Vacuum* **1985**, *35*, 67.
(3) Kaesz, H. D.; Williams, R. S.; Hicks, R. F.; Zink, J. I.; Chen, Y.; Müller, H.; Xue, Z.; Xu, D.; Shuh, D. K.; Kim, Y. K. *New J. Chem.* **1990**, *14*, 527.
(4) Vadimsky, R. G.; Frankenthal, R. P.; Thompson, D. E. *J. Electrochem. Soc.* **1979**, *126*, 2017.
(5) Donoval, D.; Stolt, L.; Norde, H.; Pires, J. D. S.; Tove, P. A.; Petersson, C. S. *J. Appl. Phys.* **1982**, *53*, 5352.
(6) Aspnes, D. E.; Heller, A. *J. Vac. Sci. Technol. B* **1983**, *1*, 602.
(7) Green, M. L.; Gross, M. E.; Papa, L. E.; Schnoes, K. J.; Brasen, D. *J. Electrochem. Soc.* **1985**, *132*, 2677.
(8) Chang, Y. S.; Chou, M. L. *J. Appl. Phys.* **1990**, *68*, 2411.
(9) Chang, Y. S.; Chou, M. L. *J. Appl. Phys.* **1991**, *69*, 7848.
(10) Myburg, G.; Auret, F. D. *Appl. Phys. Lett.* **1992**, *60*, 604.
(11) Myburg, G.; Barnard, W. O.; Meyer, W. E.; Auret, F. D.; Burger, H. *Thin Solid Films* **1992**, *213*, 113.
(12) Barnard, W. O.; Myburg, G.; Auret, F. D. *Appl. Phys. Lett.* **1992**, *61*, 1933.
(13) Grill, A.; Kane, W.; Viggiano, J.; Brady, M.; Laibowitz, R. *J. Mater. Res.* **1992**, *7*, 3260.
(14) Emsley, J. *The Elements*; Clarendon Press: Oxford, 1989; p 251.
(15) Parkin, S. S. P.; Morr, N.; Roche, K. P. *Phys. Rev. Lett.* **1990**, *64*, 2304.
(16) Viguié, J. C.; Spitz, J. *J. Electrochem. Soc.* **1975**, *122*, 585.
(17) Crosby, J. N.; Hanley, R. S. U.S. Patent, 1981.
(18) Trent, D. E.; Paris, B.; Krause, H. H. *Inorg. Chem.* **1964**, *3*, 1057.
(19) Lehwald, S.; Wagner, H. *Thin Solid Films* **1974**, *21*, S23.
(20) Gagné, M. R.; Takats, J. *Organometallics* **1988**, *7*, 561.
(21) Senzaki, Y.; McCormick, F. B.; Gladfelter, W. L. *Chem. Mater.* **1992**, *4*, 747.

0897-4756/93/2805-1715$04.00/0

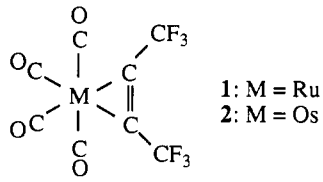

1: M = Ru
2: M = Os

Experimental Section

In general, preparations and manipulations of precursors were performed under a purified nitrogen atmosphere using standard Schlenk techniques. $Ru_3(CO)_{12}$ and OsO_4 were used as purchased from Strem Chemicals Inc. Hexafluoro-2-butyne was purchased from PCR Inc. Carbon monoxide from Air Products, hydrogen from GenEx, and nitrogen from Northern Cryogenics were used as carrier gases as received. Pentane and toluene were distilled over sodium/benzophenone prior to use. Auger electron spectra (AES) were measured on Physical Electronics PHI Model548 and PHI Model 595 electron spectrometers. X-ray photoelectron spectroscopy (XPS) analyses were carried out on Physical Electronics PHI Model 5400 ESCA system with Mg Kα X-ray source operated at 15 kV and 300 W. All binding energies were referenced to Au $4f_{7/2}$ at 84.0 eV. The curve fit of the spectra was conducted using PHI 5000 series ESCA system, Model 8503A, version 3.0 B. AES and XPS data of thin films were collected after Ar^+ sputtering of the film surface for 2 min. Scanning electron micrographs (SEM) were obtained on a Hitachi S-900 field emission scanning electron microscope without any additional metal coatings on samples to improve conductivity. Film thicknesses were determined by stylus profilometry (Dektak IIA), and resistivities were measured at 25 °C by a Veeco FPP-5000 four-point probe. X-ray diffraction analyses were obtained using a Rigaku D-MaxII diffractometer with Cu Kα radiation. Infrared spectra were obtained on a Mattson Polaris FTIR spectrometer. ^1H, ^{13}C, and ^{19}F NMR spectra were obtained on an IBM AC-300 and Varian VXR-300 spectrometer. Electron impact mass spectra were collected on a Finnigan 4000 instrument. Gas chromatography/mass spectrometry (GC-MS) data were collected on a Finnigan MAT95 instrument. Elemental analyses were performed by Galbraith Laboratories, Inc.

The CVD reactor employed in the low-pressure chemical vapor deposition was a hot-wall quartz reactor system equipped with a precursor pot, a mechanical pump, a furnace, and a U-tube trap. For the use of carrier gases, a flow meter, a mercury manometer, and flow restricter (12 mm diameter 4–8-μm glass frit) were added to the system as shown in Figure 1. The reactor tube was made of quartz with an inside diameter of 2.6 cm and a length of 35 cm. The temperature reported for a deposition was determined using a thermocouple located outside the tube below the substrates at 4.0 cm from the edge of the furnace. The substrates, Si(100) wafers, were degreased and etched prior to use by immersion in the following baths for 10 min each: tetrachloroethane, methanol, distilled water, dilute HF, and distilled water. The substrates were placed parallel to the gas flow at several locations within the constant-temperature region in the reactor tube toward the entrance to the reactor. A profile of the furnace with the reactor tube established that a reasonably constant temperature was achieved 2–3 cm from the beginning edge of the heating coils. The relative accuracy of the temperatures reported is estimated to be 5%.

Preparation of Ru(hfb)(CO)$_4$ (1). Ru(hfb)(CO)$_4$ was prepared according to the method described in ref 20 with a slight modification as follows. Triruthenium dodecacarbonyl (0.65 g) in 65 mL of freshly distilled pentane was reacted with 100 atm of CO in an autoclave at 150 °C for 10 h.[22,23] The product of this reaction, $Ru(CO)_5$, in pentane was transferred to a 100-mL quartz flask equipped with a cooling jacket. Hexafluoro-2-butyne (1.5 g) was condensed into the solution at −25 °C, and the solution was irradiated using filtered wavelengths longer than 370 nm for 8 h with constant stirring and cooling at −25 °C. The reaction solution was warmed to 0 °C, and the solvent was removed at a pressure of 20 Torr. The final product (0.69 g, 60% yield) was obtained as white crytals following sublimation (0.05 Torr, 25 °C). Although 1 is stable at 25 °C, it should be kept cold during storage.

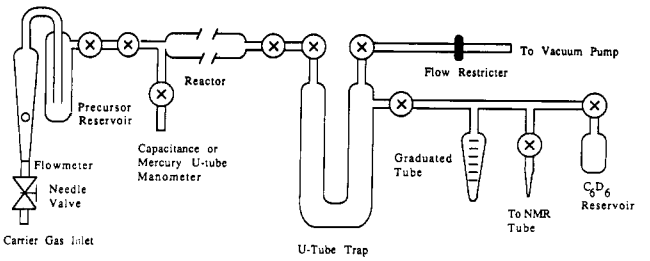

Figure 1. CVD reactor system.

Preparation of Os(hfb)(CO)$_4$ (2). Os(hfb)(CO)$_4$ was prepared according to the method described in a literature[20] with a slight modification as follows. Osmium tetraoxide (0.5 g) in 65 mL of freshly distilled pentane was reacted with 100 atm of CO in an autoclave at 160 °C for 24 h.[22,23] The pentane solution of $Os(CO)_5$ was transferred to a 100-mL quartz flask equipped with a cooling jacket. The remaining procedure was identical to that used for the preparation of Ru(hfb)(CO)$_4$ except the irradiation lasted for 10 h. The final product (0.05 g, 5.5% yield) was obtained as white crystals following sublimation (0.05 Torr, 25 °C). Although 2 is stable at 25 °C, it should be kept cold during storage.

Gas-Phase Synthesis of Ru$_2$[μ-η^1:η^1:η^4-C$_4$(CF$_3$)$_4$](CO)$_6$ (3). Ru(hfb)(CO)$_4$ (0.80 g) was passed through the reactor system described above at 150 °C for 30 min under a dynamic vacuum of approximately 1 mTorr. Yellow, crystalline 3 condensed at the entrance and exit of the hot zone of the reactor. The collection of the crystals from the reactor tube using a spatula followed by recrystallization from CH_2Cl_2 at 25 °C for 7 days afforded 0.54 g of 3 (72% yield). No metal film deposition was observed. At 300 °C for 15 min, in addition to a very thin nonconductive film, 87 mg (47% yield) of 3 was formed from 200 mg of 1. Spectroscopic data of 3: IR (cm^{-1}, pentane) 2117 (m), 2096 (s), 2064 (s), 2054 (s), 2037 (s), 2021 (w); ^{19}F NMR (ppm from $CFCl_3$, CD_2Cl_2) −45.2 (br s, 6F), −51.1 (br s, 6F); ^{13}C NMR (ppm, CD_2Cl_2) 121.6 (q, J_{C-F} = 280.8 Hz), 126.5 (q, J_{C-F} = 274.6 Hz), 138.8 (s), 139.3 (s), 189.90–190.5 (br). Anal. Calcd: C, 24.22; H, 0.00. Found: C, 24.23; H, <0.5. EI mass spectrum m/e = 696 for parent ion $Ru_2C_{14}O_6F_{12}^+$ followed by fragments corresponding to loss of 6 CO ligands; mp 139–140 °C.

Synthesis of Ru$_2$[μ-η^1:η^1:η^4-C$_4$(CF$_3$)$_4$](CO)$_6$ (3) in Toluene. Ru(hfb)(CO)$_4$ (10 mg) and 5 mL of dry toluene were placed in a 50-mL Pyrex thick-wall tube and heated to reflux with stirring. Within 10 min the reaction solution turned yellow. After refluxing and stirring for 3 h, the mixture was cooled to room temperature. Following removal of the solvents under vacuum, yellow solid 3 (7 mg, 76% yield) was isolated.

Gas-Phase Synthesis of Os$_2$[μ-η^1:η^1:η^4-C$_4$(CF$_3$)$_4$](CO)$_6$ (4). Os(hfb)(CO)$_4$ (26 mg) was passed through the reactor system described above at 200 °C for 3 min under a dynamic vacuum of approximately 1 mTorr. This afforded brownish white, crystalline 4, which condensed at the entrance and exit of the hot zone of the reactor tube (2 mg, 8% yield). No recrystallization was attempted. Spectroscopic data: IR (cm^{-1}, CH_2Cl_2) 2120 (m), 2093 (s), 2057 (m), 2035 (m), 2012 (m); ^{19}F NMR (ppm from $CFCl_3$, CD_2Cl_2) −45.7 (br s, 6F), −50.8 (br s, 6F). Anal. Calcd: C, 19.27; H, 0.00. Found: C, 19.27; H, <0.5. EI mass spectrum m/e = 873 for parent ion $Os_2C_{14}O_6F_{12}^+$ followed by fragments corresponding to loss of six CO ligands; mp 125–127 °C.

CVD of Ru and Os Thin Films without a Carrier Gas. The reactor system described above was evacuated and the Si-(100) substrates were heated in the reactor tube to the deposition temperature for 30 min prior to the deposition. The depositions were performed without a carrier gas under a dynamic vacuum of approximately 1 mTorr. The precursor temperature was 25 °C for 1 and 2. For the use of ruthenium dimer 3, the precursor and the glass adapter connected to the reactor tube were heated to 65 °C by wrapping with a heating tape to prevent condensation of the precursor.

(22) Calderazzo, F.; Léplattenier, F. *Inorg. Chem.* **1967**, *6*, 1220.
(23) Whyman, R. *J. Organomet. Chem.* **1973**, *56*, 339.

Table I. Deposition Conditions on Si(100) and Film Properties

film no.	precursor and temp (°C)	dep temp (°C)	carrier gas, pressure (Torr)	dep time (min)	growth rate (nm/min)	resistivity (μΩ cm)	grain size[a] (nm)	comments
1	1 (25)	500	none (0.001)	3	60	160	30	*b*
2	1 (25)	500	H_2 (500)	5	21	22	60	*c*
3	1 (25)	500	H_2 (250)	5	30	38	50	*c*
4	1 (25)	500	H_2 (115)	5	32	51	30	*c*
5	1 (25)	400	H_2 (250)	5	32	85	60	*c*
6	1 (25)	300	H_2 (250)	10	12	91	15–60	*c*
7	1 (25)	200	H_2 (250)	10	4	192	15	*c, d*
8	1 (25)	300	N_2 (250)	10	47	698	15	*b, d*
9	3 (65)	500	none (0.001)	60	4	440	30	*b*
10	3 (65)	500	H_2 (135)	20	10	113	25	*c*
11	3 (65)	600	H_2 (135)	30	10	69	30	*c*
12	2 (25)	600	none (0.001)	10	15	750	20	*b*
13	2 (25)	600	H_2 (25)	10	14	81	20	*c*

[a] Measured by SEM. [b] Amorphous with a marginal degree of crystallinity. [c] Polycrystalline. [d] Formation of measurable amounts of 3.

CVD of Ru and Os Thin Films with H_2. A mercury manometer, a flow meter, and pressure restrictor were attached to the CVD reactor system as described above. The reactor system was evacuated, and the substrates were heated in the reactor tube to the deposition temperature for 30 min prior to the deposition. The precursor temperature was 25 °C for 1 and 2. The depositions were performed by passing H_2 through the precursor pot containing 1 or 2 with a flow rate of 300 sccm or greater for the H_2 partial pressure of 250 Torr. A precise flow rate measurement was not possible because the actual flow rate exceeded the scale of the flow meter. For the use of ruthenium dimer 3, the precursor pot and the glass adapter connected to the reactor tube were heated to 65 °C by wrapping with a heating tape to prevent condensation of the precursor. H_2 carrier gas was passed through the precursor pot containing 3 with a flow rate of 165 sccm for the H_2 partial pressure of 135 Torr.

Vapor Pressure Measurement of 1. A Schlenk tube containing 1 was equipped with a capacitance manometer and a stopcock adapter and evacuated to approximately 1 mTorr with liquid nitrogen cooling. The manometer was isolated from the flask and the temperature was stabilized at 25 °C. By opening the stopcock to the manometer, the system was backfilled with the partial pressure of 1. The vapor pressure was monitored for 20 min. This procedure was repeated three times, and the average vapor pressure of 1 was 1.5 Torr.

Trapping of Gas Byproducts in the CVD of Ru and Os Thin Films. A U-tube filled with glass beads was attached to the exit of the reactor tube. The volatile byproducts were trapped in the liquid nitrogen cooled U-tube, then distilled into an NMR tube which was sealed under vacuum. After obtaining NMR spectra, the contents of the tube were further analyzed by GC-MS.

Results

The deposition conditions on Si(100) substrates and the resulting film properties are summarized in Table I. Compounds 1 and 2 are stable solid mononuclear metal carbonyl complexes with the vapor pressure of 1.5 Torr at 25 °C for 1 and a slightly lower vapor pressure for 2.

Description of Film Deposition. Under vacuum conditions, metallic ruthenium and osmium film deposition occurred in the region 2–7 cm downstream of the edge of the furnace heating coils. The temperature listed in Table I corresponds to the constant-temperature region approximately 2 cm from the beginning edge of the heating coils on the furnace. Osmium film deposition from 2 occurred in the region 1–2 cm closer to the center of the reactor tube than ruthenium film deposition from 1. The film growth rate of ruthenium (60 nm/min at 500 °C, film no. 1) was significantly higher than that of osmium (15 nm/min at 600 °C, film no. 12), which may be due in part to the difference in volatilities between 1 and 2.

The use of H_2 carrier gas induced the depositions at the beginning of the heating coil region to 5–6 cm. The films deposited at the entrance region of the reactor (where the temperature was significantly lower than the constant deposition temperature toward the center of the reactor tube) exhibited a rough morphology and were nonadhesive. The films employed for characterization were from the constant-temperature region of the reactor. While H_2 carrier gas was passed through the precursor pot, no change in appearance of the precursors was noted during the deposition experiments.

Composition of the Films. Auger electron spectroscopy (AES) and X-ray photoelectron spectroscopy (XPS) were used to determine the composition of the films. Ater sputtering through the top layer of a film grown at 500 °C under vacuum (film no. 1), a survey AES spectrum showed no signal attributable to fluorine. Slow scans over the regions of interest revealed an oxygen content of 1%. Due to the overlap between the carbon KLL line at 271 eV and the ruthenium MNN line at 273 eV, a direct measurement of the carbon content was not possible. In previous studies, a comparison of the difference in the intensities of the ruthenium transitions located at 273 and 231 eV relative to ruthenium standards was used as a gauge of the carbon content. For pure ruthenium, the reported value of I_{273}/I_{231} and 2.64.[7] In the films grown using Ru(hfb)$(CO)_4$, the observed ratio of 2.64 suggested that the carbon content was below the limits of detection. The uncertainty of this method of carbon analysis, however, prompted us to find an alternative procedure.

Figure 2a,b shows the Ru 3d region of the XPS spectra of films grown at 500 °C with H_2 carrier gas and under vacuum (film nos. 3 and 1, respectively). The binding energies at 280.0 and 284.1 eV correspond to Ru $3d_{5/2}$ and Ru $3d_{3/2}$, respectively.[24,25] In Figure 2a the peak intensity ratio of 61:39 is in accordance with the theoretical value of 3:2.[26] If carbon were present in this film, the observed ratio would reflect this. By requiring that the theoretical ratio between the $3d_{5/2}$ and $3d_{3/2}$ peaks maintained in Figure 2b, we observed that an additional peak centered at 284.4 eV must be added to achieve a satisfactory curve fit to the spectrum. This peak was located at the position expected for the carbon 1s peak and corresponds to approximately 20 atom % of carbon.

(24) Kim, K. S.; Winograd, N. *J. Catalysis* **1974**, *35*, 66.
(25) *Handbook of X-ray Photoelectron Spectroscopy*; Muilenburg, G. E., Ed.; Perkin-Elmer: Eden Praire, 1979; p 190.
(26) Feldman, L. C.; Mayer, J. W. *Fundamentals of Surface and Thin Film Analysis*; North-Holland: New York, 1986; p 354.

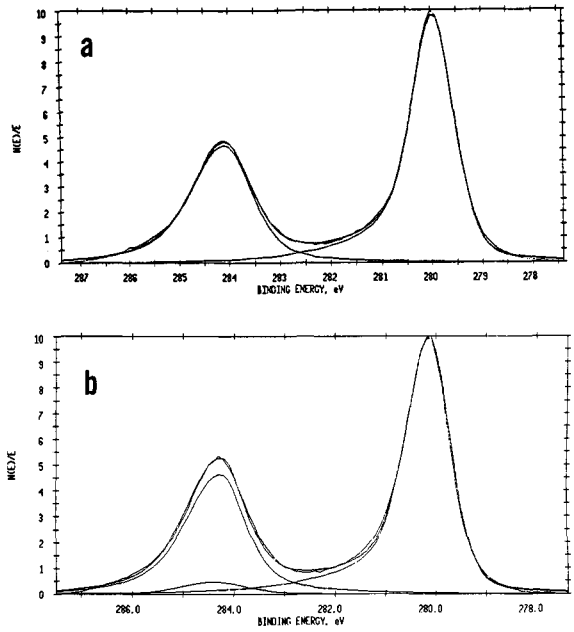

Figure 2. Experimental and fitted XPS of (a) Ru 3d region of film no. 3 (deposition temperature 500 °C, H_2 pressure 250 Torr, deposition time 5 min), and (b) Ru 3d region of film no. 1 (deposition temperature 500 °C, under vacuum, deposition time 3 min).

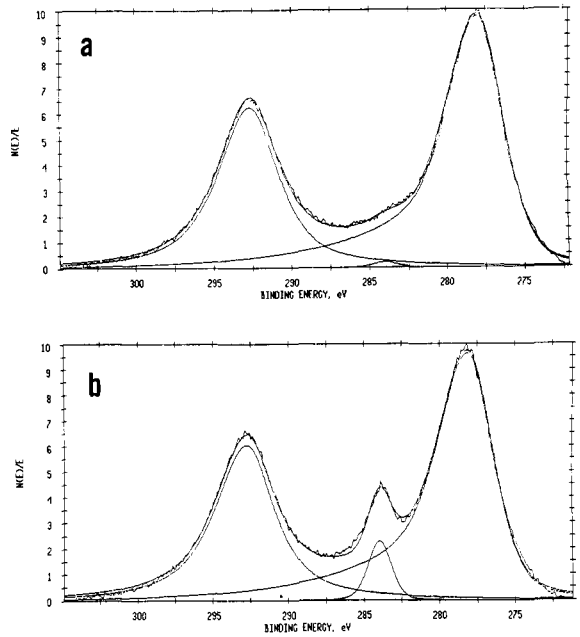

Figure 3. Experimental and fitted XPS of (a) Os 4d region of film no. 13 (deposition temperature 600 °C, H_2 pressure 250 Torr, deposition time 10 min), and (b) Os 4d of film no. 12 (deposition temperature 600 °C, under vacuum, deposition time 10 min).

The XPS spectra of the osmium films deposited at 600 °C with H_2 carrier gas (film no. 13) and without carrier gas (film no. 12) are shown in Figure 3a,b, respectively. The $4d_{5/2}$ and $4d_{3/2}$ of metallic Os have binding energies of 278.5 and 293.1 eV referenced to Au $4f_{7/2}$ at 84.0 eV full width at half-maximum (fwhm) of 4.1 eV.[27] Both the binding energies and the line widths of the peaks at 278.0 eV (fwhm = 4.0 eV) and 292.6 eV (fwhm = 4.2 eV) in Figure 3a and the peaks at 278.2 eV (fwhm = 4.0 eV) and 292.8 eV (fwhm = 4.3 eV) in Figure 3b were consistent with the assignment and $4d_{5/2}$ and $4d_{3/2}$ of osmium metal. The peak intensity ratio of 60:39 in Figure 3a and 58:38 in Figure 3b) were also consistent with the theoretical value of 3:2 for Os $4d_{5/2}$:Os $4d_{3/2}$. In Figure 3b a distinct peak located at 284.0 eV was assigned to carbon. This assignment was consistent with the detection of carbon in the AES spectrum. When the osmium film was grown in the presence of H_2, this peak was greatly diminished in intensity (Figure 3a). The XPS analyses provided the composition ratio of the films as follows: Os 87%, 5% C, and 8% O for film no. 13; 55% Os, 42% C, and 3% O for film no. 12. Fluorine content was below the detection limit by XPS in both films.

Film Microstructure, Crystallinity, and Resistivity. The metal films deposited on Si(100) substrates in the absence of carrier gas at 500 °C (film no. 1) for Ru or 600 °C for Os (film no. 12) were smooth and reflective to visual inspection and had a slightly dark color. Examination of the surface using scanning electron microscopy (SEM) revealed that the grain size was 20 nm for the Ru films. X-ray diffraction (XRD) established that the coherent length of Ru grains, estimated using Scherrer equation, was 3.3 nm (4 nm for Os). Close examination of the micrographs (Figure 4 for Ru) suggested that both the Ru and Os films exhibited a porous, granular structure. Measurement of the resistivity of the films by four-point probe gave a value of 160 $\mu\Omega$ cm, at best, for Ru and 750 $\mu\Omega$ cm for Os. We attributed these relatively high values to the porous microstructure suggested from the SEM analysis, to the carbon impurities indicated by the XPS analysis, and to the low crystallinity observed in XRD.

For both metals, the use of H_2 as a carrier gas for the deposition of thin films on Si(100) substrates enhanced the purity, crystallinity, and conductivity of the films. The resulting films (film no. 2, no. 3, and no. 4 for Ru and no. 13 for Os) were smooth and highly reflective with good adhesion to the substrates and had a color nearly identical to that of the silicon substrate. Figure 5 shows the SEM pictures of film no. 3 which has densely packed crystalline microstructure. The grain size of the Ru films, determined from SEM analyses, increased from 30 to 60 nm as the partial pressure of H_2 gas increased from 115 to 500 Torr. The grain size (by SEM) of the Os films increased to 20 nm for depositions conducted under H_2 at 600 °C. The XRD patterns shown in Figure 6 demonstrated the effect of H_2 carrier has on the crystallinity of the metal films. The coherent lengths measured from these data for Ru were typically 19–26 and 13 nm for Os. The resistivities of the Ru films deposited at 500 °C with H_2 carrier gas ranged between 22 and 51 $\mu\Omega$ cm, which compared to the resistivity of bulk ruthenium of 7.6 $\mu\Omega$ cm at 0 °C. For Os films deposited at 600 °C in the presence of H_2 carrier gas, the resistivity was 81 $\mu\Omega$ cm (the value for bulk osmium is 8.1 $\mu\Omega$ cm at 0 °C). Polycrystalline ruthenium films could also be deposited at temperatures as low as 300 °C in the presence of H_2 (film no. 6); however, the resistivity of the films increased as the deposition temperature was lowered. Also lower film growth rates were observed at lower deposition temperatures. By using N_2 as a carrier gas at 300 °C, dark metallic films with low crystallinity and high resistivity were obtained (film no. 8). In addition, the formation of dimers 3 (see below) was observed. At 200 °C (film no. 7), the deposition under H_2 resulted in films with low crystallinity and the formation of a small

(27) Berndtsson, A.; Nyholm, R.; Martensson, D.; Nilsson, R.; Hedman, J. *Phys. Status Solidi B* **1979**, *93*, K103.

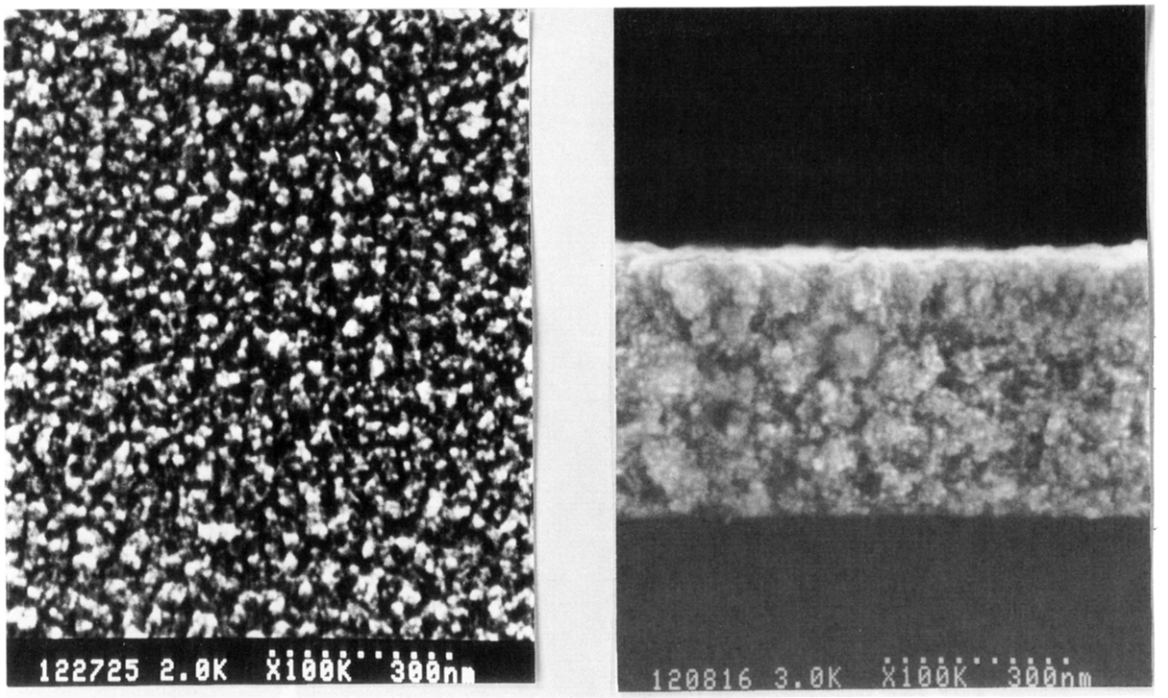

Figure 4. SEM of film no. 1 (deposition temperature 500 °C, under vacuum, deposition time 10 min) showing a plan (left) and cross sectional (right) view.

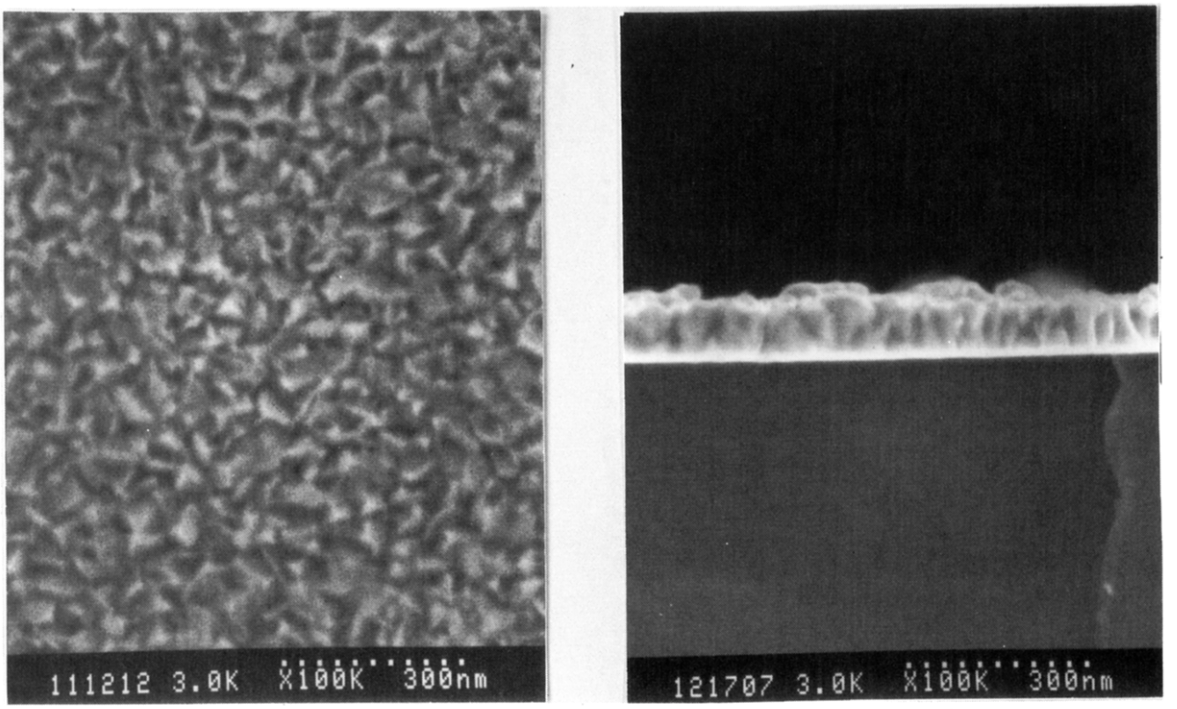

Figure 5. SEM of film no. 3 (deposition temperature 500 °C, H_2 pressure 250 Torr, deposition time 5 min) showing a plan (left) and cross-sectional (right) view.

amount of **3**. That polycrystalline ruthenium thin films can be obtained at the deposition temperature as low as 300 °C under H_2 prompted us to use various thermally sensitive substrates. Reflective polycrystalline metallic thin films were successfully grown on polyimide and glass substrates under the deposition conditions at 300 °C for 10 min using H_2 carrier gas (250 Torr).

Volatile Byproducts of the Deposition. When the deposition was conducted at low temperature (300 °C) under vacuum (1 mTorr), the thickness of the film was notably decreased and a yellow crystalline solid was condensed at both the entrance and exit of the reactor. At 150 °C, no film deposition occurred and a larger quantity of the yellow solid was isolated. The new compound, **3**,

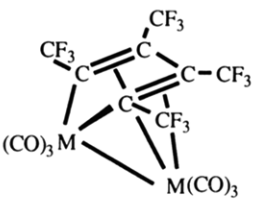

3: M=Ru
4: M=Os

was completely characterized using analytical and spectroscopic methods and, ultimately, by single-crystal X-ray

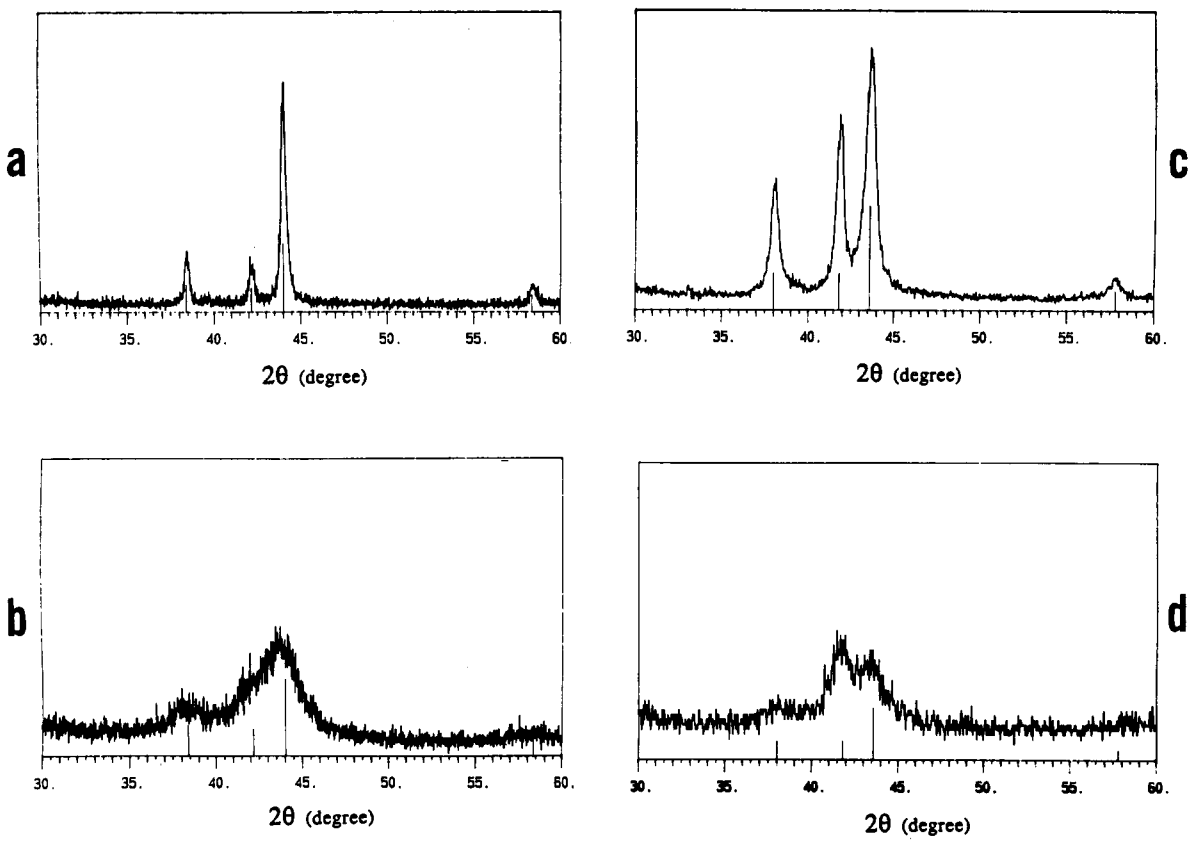

Figure 6. X-ray diffraction pattern of (a) film no. 3 (deposition temperature 500 °C, H_2 pressure 250 Torr, deposition time 5 min), (b) film no. 1 (deposition temperature 500 °C, under vacuum, deposition time 10 min), (c) film no. 13 (deposition temperature 600 °C, H_2 pressure 250 Torr, deposition time 10 min), and (d) film no. 12 (deposition temperature 600 °C, under vacuum, deposition time 10 min).

crystallography.[21] The structure of $Ru_2[\mu\text{-}\eta^1\text{:}\eta^1\text{:}\eta^4\text{-}C_4(CF_3)_4](CO)_6$, results from loss of CO and coupling of the alkyne ligands from 2 equiv of $Ru(hfb)(CO)_4$. Although within the iron triad numerous examples of this structural type are known,[28-31] the gas-phase dimerization of this kind is unprecedented. The surprisingly high yields (47% at 300 °C; 72% at 150 °C) formed during this flash vacuum pyrolysis demonstrate the stability of the dimer and the synthetic utility of this reaction. The dimer **3** can also be synthesized by refluxing a toluene solution of **1** for 3 h.

Analogously, the flash vacuum pyrolysis of **2** at 200 °C afforded the dinuclear complex $Os_2[\mu\text{-}\eta^1\text{:}\eta^1\text{:}\eta^4\text{-}C_4(CF_3)_4](CO)_6$ (**4**) in 8% yield. No attempts were made to optimize the yield. The new compound, **4**, was characterized using analytical and spectroscopic methods. As with the ruthenium dimer **3**, the elemental analysis, the mass spectrum, the IR stretching bands of carbonyl groups, and the ^{19}F NMR spectrum were consistent with the structure of $Os_2[\mu\text{-}\eta^1\text{:}\eta^1\text{:}\eta^4\text{-}C_4(CF_3)_4](CO)_6$.

Although the volatility of dimer **3** was significantly less than monomer **1**, ruthenium films can be grown on Si(100) substrates at 500–600 °C using **3** as the precursor provided the precursor pot and lines were heated to 65 °C. The resulting dark metallic films (film no. 9) were adhesive to the substrates and visually smooth and reflective. The grain size of 30 nm from SEM and the resistivity of 440 $\mu\Omega$ cm were observed for the deposition conducted at 500 °C under vacuum. Similar to the case of the deposition from monomer **1**, the use of H_2 as a carrier gas enhanced the purity, crystallinity, and conductivity of the resulting films. The coherent length estimated from XRD increased from 2.7 (film no. 9) to 15 nm (film no. 10) and 21 nm (film no. 11).

The NMR and GC-MS analyses of the gaseous byproducts established that the majority of the condensable material from **1** was hexafluoro-2-butyne (m/e = 162, ^{19}F NMR δ = −53.2 ppm from $CFCl_3$ in C_6D_6) when the deposition was conduced under vacuum at 500 °C. The gas chromatogram showed the elution of two smaller, less well-resolved peaks immediately following the elution of hexafluoro-2-butyne. The highest mass values for these two peaks were m/e = 362 and 324, respectively. These values and the associated fragmentation patterns corresponded to the formulas C_8F_{14} and C_8F_{12}. Although we cannot assign specific structures to these formulas, the fact that they have exactly twice the numbers of carbons as hfb suggests that they may arise from compound **3**.

When the deposition was conducted from **1** using H_2 as carrier gas at the temperature range 300–500 °C, the major condensable gas product was hexafluoro-2-butene as indicated by a m/e value of 164 in GC-MS and the olefinic protons (δ = 4.96 and 5.60 ppm from TMS in C_6D_6) in the ^1H NMR spectrum. No hexafluoro-2-butyne was detected by either GC-MS or ^{19}F NMR. Also, no hexafluorobutane was observed. The gas chromatogram showed the ap-

(28) Nesmeyanov, A. N.; Rybinskaya, M. I.; Rybin, L. V.; Kaganovich, V. S. *J. Organomet. Chem.* **1973**, *47*, 1.
(29) Fehlhammer, W. P.; Stolzenberg, H. In *Comprehensive Organometallic Chemistry*; Wilkinson, G., Stone, F. G. A., Abel, E. W., Eds.; Pergamon Press: Oxford, 1982; Vol. 4, p 513.
(30) Adams, R. D.; Selegue, J. P. In *Comprehensive Organometallic Chemistry*; Wilkinson, G., Stone, F. G. A., Abel, E. W., Eds.; Pergamon: Oxford, 1982; Vol. 4, p 967.
(31) Seddon, E. A.; Seddon, K. R. *Chemistry of Ruthenium*; Elsevier: Amsterdam, 1984; p 1373.
(32) Templeton, J. L. *Adv. Organomet. Chem.* **1989**, *29*, 1.

Scheme I. Proposed Ru Deposition Mechanism From Ru(hfb)(CO)$_4$

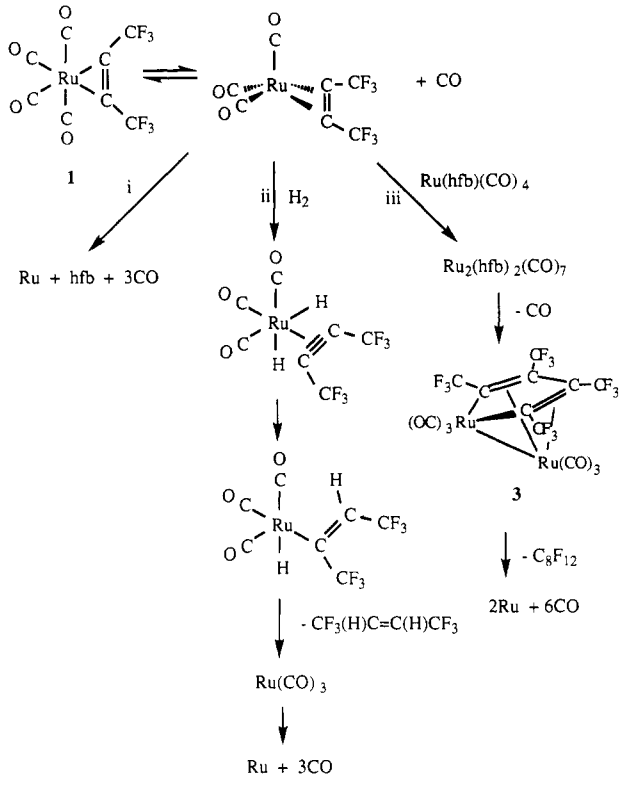

pearance of a smaller peak following the elution of hexafluoro-2-butene. The highest mass value for this peak was m/e = 308. This value and the associated fragmentation patterns corresponded to the formula $C_8F_{11}H_3$ as minor component. This formula may be derived from the partial hydrogenation (+4H) of C_8H_{12} species followed by dehydrofluorination (–HF) possibly from fragmentation in the mass spectrometer. As with the above-mentioned case, the fact that it has exactly twice the numbers of carbons as hfb suggests that it may arise from hydrogenation of 3.

Discussion

Several observations about the chemical vapor deposition of ruthenium offer insight into the mechanism of the reaction. First, the low-temperature limit for Ru deposition from $Ru(CO)_4[C_2(CF_3)_2]$ (1) is controlled by the increasing importance of a competing reaction pathway; the formation of the dinuclear species. A total of two CO ligands are lost during the formation of $Ru_2[C_4(CF_3)_4](CO)_6$ (3), and we suggest that CO dissociation precedes dimer formation. Second, the observation that this reaction occurs in toluene solution as well as in the CVD reactor provides strong evidence that the surface is not involved in this transformation. Third, using hydrogen as a carrier gas results in a substantial (nearly quantitative) reduction in the amount of $Ru_2[C_4(CF_3)_4](CO)_6$ (3) formed even when the deposition is conducted at low temperatures where dimer formation was prevalent under vacuum conditions.

Scheme I shows the proposed explanation of these observations. Dissociation of CO from $Ru(CO)_4[C_2(CF_3)_2]$ (1) may be facilitated by the ability of alkyne ligands to act as either a two- or four-electron donors.[32] In the absence of dimer formation, this intermediate further decomposes directly to give ruthenium metal (path i). At temperatures below 400 °C the lifetime of $Ru(CO)_3[C_2(CF_3)_2]$ is apparently long enough to allow it to collide and react with another monomer, presumably the more abundant starting material $Ru(CO)_4[C_2(CF_3)_2]$ (1, path iii). This reaction occurs, at least to some extent, at temperatures above 400 °C, but at these temperatures $Ru_2[C_4(CF_3)_4](CO)_6$ (3) also forms ruthenium films. It is unlikely that all the deposited ruthenium forms from the dimer. If we assume that ruthenium deposition from $Ru_2[C_4(CF_3)_4](CO)_6$ (3) is responsible for the formation of alkyne dimers, C_8F_{12} and C_8F_{14}, and that the quantity of $C_2(CF_3)_2$ present is indicative of the direct deposition from the monomer, then most of the CVD occurs directly from the monomer.

Hydrogen is apparently able to trap $Ru(CO)_3[C_2(CF_3)_2]$ to give an intermediate dihydride which can cleanly eliminate the alkene by a sequence of standard reactions (path ii). Following the reductive elimination of $C_2H_2(CF_3)_2$, the coordinately unsaturated fragment $Ru(CO)_3$ may react with the surface to give metallic ruthenium. It could also react with H_2 but at these temperatures this species would also likely form ruthenium metal. The observation that no free $C_2(CF_3)_2$ is formed during the deposition with H_2 present suggests that path ii in Scheme I is efficient. One alternative explanation for the lack of observation of the alkyne is that the metal surface catalytically hydrogenates the alkyne. If this reduction were occurring, we would expect to see some further reduction to give $CF_3CH_2CH_2CF_3$. No evidence of this species was found during the deposition.

Films grown in the absence of hydrogen contained significant amounts of carbon. Ruthenium is one of the most active catalysts for the Fischer–Tropsch reaction (CO + H_2 → organics).[33] Many of these catalysts function through a carbide intermediate which can be removed upon hydrogenation. The dissociative chemisorption of CO on the growing ruthenium (or osmium) surface can explain the incorporation of carbon into the films. In the absence of H_2, the oxygen could be removed from the surface by its combination with CO to give CO_2. Overall, the source of the carbon can be represented by the disproportionation of CO (eq 1).

$$2CO \rightarrow C + CO_2 \quad (1)$$

The composition and microstructure of the films were dependent upon which path in Scheme I was available. It is likely that the reduced crystallinity and the porous structure of the films grown in the absence of hydrogen (path i) are caused by the carbon contamination. The films grown at the same temperatures under hydrogen (path ii) exhibit a much greater degree of crystallinity and density and display much lower resistivities.

Acknowledgment. This work was funded by the Center for Interfacial Engineering, a NSF Engineering Research Center, and the Graduate School of the University of Minnesota. We would like to thank Chris D. Frethem (Department of Cell Biology and Neuroanatomy, University of Minnesota) for his assistance with the cross-sectional SEM, Dezhong Liu (Surface Analysis Center, University of Minnesota) for his assistance with the XPS, and Ed Larka (Department of Chemistry, University of Minnesota) for the MS analyses.

(33) Vannice, M. A. *J. Catal.* **1975**, *37*, 449.